

A novel edge detection method based on 2-D Gabor wavelet

Chunya Tong*

School of Electronic and Information Engineering, Ningbo University of Technology, Ningbo, Zhejiang, 315016, China

Received 1 July 2014, www.tsi.lv

Abstract

With the features of substantial data and complex landmark, remote sensing images need a higher requirement for edge detection operator. Due to the limitations of grads operator and Canny operator in edge detection, this paper presents an edge detection method based on 2-D Gabor wavelet real part and the experimental analysis shows this method was better on edge detection.

Keywords: edge detection, 2-D Gabor wavelet, real part, remote sensing images

1 Introduction

Edge detection is the first step of analysing and understanding the image, and also is the part of image pre-processing, which is the key to dealing with many complex issues [1]. Because aerial remote sensing images have access to convenience as well as high resolution, important buildings' edge information can be obtained through edge detection. However, since that remote sensing image has large amounts of data and contains abundant information, it needs a better operator for edge detection.

Now there are some frequently-used nonlinear operators like Grads operator, Laplace operator, LOG operator, Sobel operator, Prewitt operator, Robert operator, Canny operator, direction operator and etc. Besides, there are linear operators like surface fitting and so on [2, 4]. These operators have different characteristics: Grads operators is similar to high-pass filtering, only works in sharpening the edge; Sobel operator is a kind of weighted average operator and it weighted the point near the centre to stress its edge; Robert grads operator is sensitive to noise, so it is rarely used for detecting dense point region edge. Laplace operator is rotation invariant in detecting edge, which is called isotropic. Compared with the edge, it responds stronger to the corner, the endpoint and isolated points; before the LOG operator does differential operator, firstly it smoothest image processing to reduce the noise. Therefore, it relieves the issue that differential operator is sensitive to noise yet influences the result of edge detecting. Canny operator, owing to its strictness with the setting of parameters, is conducive to automated processing of image data. Due to a variety of deficiencies of the algorithms above, it is difficult to be applied to detect the edge of remote sensing images successfully, which contain a large amount of complex landmark. Thus, this paper put forward a novel edge detection method based on 2-D Gabor wavelet.

2 2-D Gabor wavelet transform

2.1 2-D GABOR WAVELET

Being expended from one dimension of Gabor wavelet, the two dimensions Gabor wavelet is a powerful tool for multi-scale image representation and image analysis. Gabor function, as the only way to obtain the spatial and frequency domain of uncertainty relation, is often chosen as wavelet basis function [3]. The basic principle of wavelet transform is to give the representation or approximation of a signal by the convolution of the filter function with a set of signals. Function of the two-dimensional Gabor filter is a complex function, whose real parts and imaginary parts can be expressed as follows:

$$\text{Re}(\psi_j(\vec{x})) = A \times \left[\exp(\vec{k}_j \vec{x}) - \exp\left(-\frac{\delta^2}{2}\right) \right], \quad (1)$$

$$\text{Im}(\psi_j(\vec{x})) = A \times \sin(\vec{k}_j \vec{x}). \quad (2)$$

Two-dimensional Gabor wavelet's transform describes that giving a near area's grey feature of one point \vec{x} on images $I(\vec{x})$, with a convolution is defined as follows:

$$J_j(\vec{x}) = \int I(\vec{x}') \psi_j(\vec{x} - \vec{x}') d^2 \vec{x}'. \quad (3)$$

Gabor filter is a band pass filter in the spatial domain and frequency domain, which has a better ability to distinguish and a good directional selectivity in the spatial domain with good frequency selectivity in the frequency domain. Two-dimensional Gabor wavelet is easy to extract multi-scale and multi-grain direction frequency information.

* Corresponding author e-mail: 77848116@qq.com

2.2 SELECTION OF THE TWO-DIMENSIONAL GABOR FILTER BANK PARAMETERS

Parameters of two-dimensional Gabor wavelet filter bank are mainly reflected in the sampling modes of spatial and frequency domain. 2-D Gabor filter's function determines the scale by scaling and rotating a set of filters to generate its expression of the signals, and the selection of parameters is usually performed in the frequency domain. In order to sample the entire image in frequency, domain parameters of k_v , φ_μ can be chosen to represent the centre frequency and direction to describe images. Different choices of these two parameters reflect the differences in the 2-D Gabor wavelet frequency and direction of spatial sampling approach. Filter bandwidth is available from the Equation, which is expressed as follows:

$$\delta = \sqrt{2 \ln 2} \left(\frac{2^\varphi + 1}{2^\varphi - 1} \right), \tag{4}$$

where φ is half-peak bandwidth (described as octave), the relationship between φ and δ can be expressed in Table 1, where selections of the filter parameters refer to experimental data neurophysiological.

TABLE 1 Correspondence between the values of φ and δ

φ	δ
0.5	2π
1	π
1.5	2.5

The entire frequency space values from 0 to infinity. Because the actual frequency distribution of an image is a limited range, the argument k_v can be within a small range of values. Lades and his group's experiments show that for



FIGURE 2 Changes in texture direction of 2D Gabor filter function with the real part of the parameter φ_μ

Centre frequency k_v represents λ_v , the wavelength of the 2-D Gabor filters:

$$\lambda_v = \frac{2\pi}{k_v}. \tag{5}$$

When the direction parameter $\varphi_\mu = 0$, the centre frequency equals $\pi/2, \sqrt{2}\pi/4, \pi/4, \sqrt{2}\pi/8, \pi/8$, the

the image at the size of $128 * 128$, when the greatest centre frequency of the filter is $\pi/2$ and the filter bandwidth is equal to 0.5 octave, the experiment works best. As the edge of the image is randomly distributed in the range of 0 to 2π , taking into account the symmetry of the Gabor filter, the actual values is in the range of $[0, \pi]$.

For the 40 Gabor filters consists of 5 centre frequency and eight directions, when v is equal to 2, μ is equal to 4, the real and imaginary parts of 2-D Gabor filter can be represented as Figure 1.

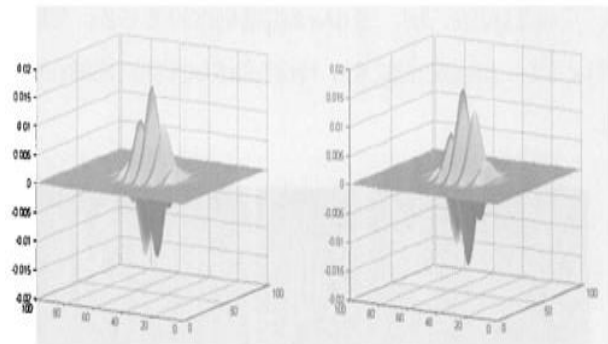


FIGURE 1 The real parts (left) and imaginary parts (right) of 2-D Gabor filter

Filter parameters φ_μ, k_v and δ represents the direction of the filter, respectively, the wavelength and the sizes of the Gaussian window. With the changes of φ_μ in the real and imaginary parts of the 2-D Gabor filter, function performs texture features in different directions.

When the centre frequency of the k is $\pi/4$, the direction parameter is $0, \pi/8, \pi/4, 3\pi/8, \pi/2$, the real parts of the filter function is shown in Figure 2.

Filters in different directions can respond to image texture features in the corresponding direction, when the image texture features are perpendicular to the direction of the filter, it makes response to the optimum.

corresponding wavelengths are: $4, 4\sqrt{2}, 8, 8\sqrt{2}, 16$. In this case, the real part of the two-dimensional Gabor filter function as shown in Figure 3. With the decrease of the centre frequency, the wavelength of filter increases. And the filter of different wavelength responds to different image features.

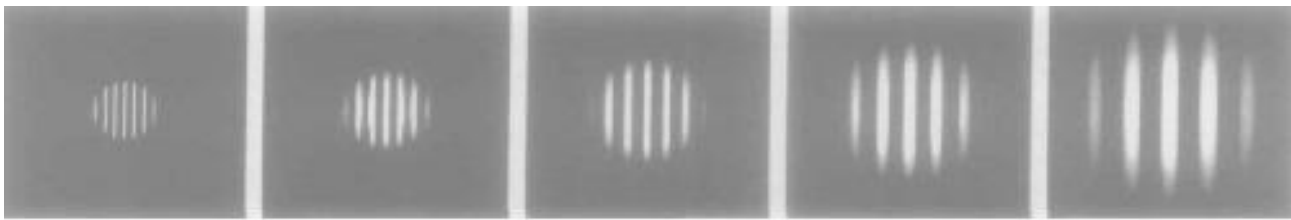


FIGURE 3 The real parts' texture direction of 2D Gabor filter function along with the changes of parameters φ_μ

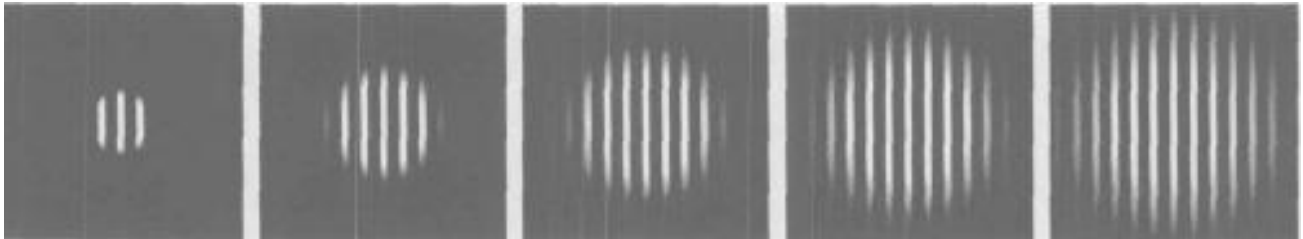


FIGURE 4 The real parts' windows of 2D Gabor filter function along with the changes of the parameter δ

$$r_v = \frac{2\sqrt{2}\delta}{k_v} \tag{6}$$

The effective radius of the Gaussian window r_v (see, Equation (6)), determines equation effective range of the image convolution. When taking centre frequency, the parameters were taken, $\pi, 2\pi, 3\pi, 4\pi, 5\pi$, the 2-D Gabor filter function can be represented in Figure 4. With the increasing Gaussian window, range of local features of a given location on the image of 2-D Gabor wavelet transform increased, but the amount of computation convolution also doubled.

3 Detecting edge method based on 2-D Gabor filters real parts

Because the real parts and imaginary parts of the two-dimensional Gabor filter are similar, for the purpose of reducing the edge detection computation, only the real parts are applied, as shown in Figure 5.

The steps are taken as follows:

- 1) Input the value of centre Frequency k_v and variance δ to determine the size of the convolution template window;
- 2) Input direction parameter φ_μ , φ_μ can be $0, 2\pi/8, \pi/4, 3\pi/8$;
- 3) Use Equation (1) to calculate the value of 2-D Gabor filter, then we have four real template's windows;
- 4) Execute convolution of the template and the image, and generate four convolution images;
- 5) Use the image of the real part to calculate the final margin, then generate four amplitude images;
- 6) Detect four magnitude of the image data in the same position, reserve maximal, then get a maximum value of the images;
- 7) Determine threshold T , and the point greater than the maximum values in the image is retained as the edge point T ;

8) Do some detailed processes for the edge point images.

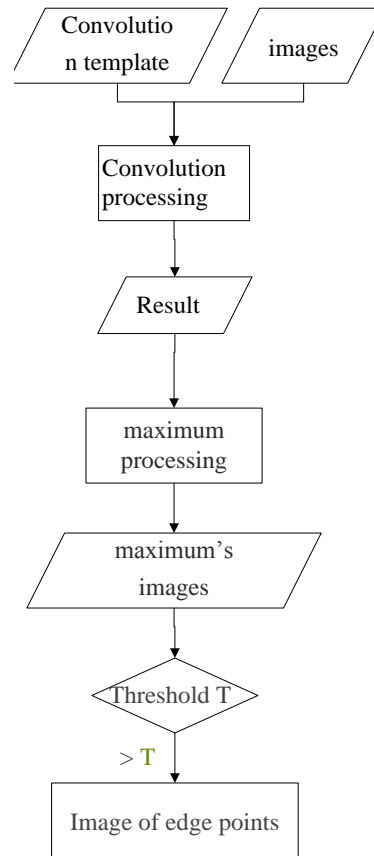


FIGURE 5 Flow chart

4 Experiments and Analysis

4.1 RESULTS BY DIFFERENT EDGE DETECTING METHOD

Edge detection results are shown in Figure 6:

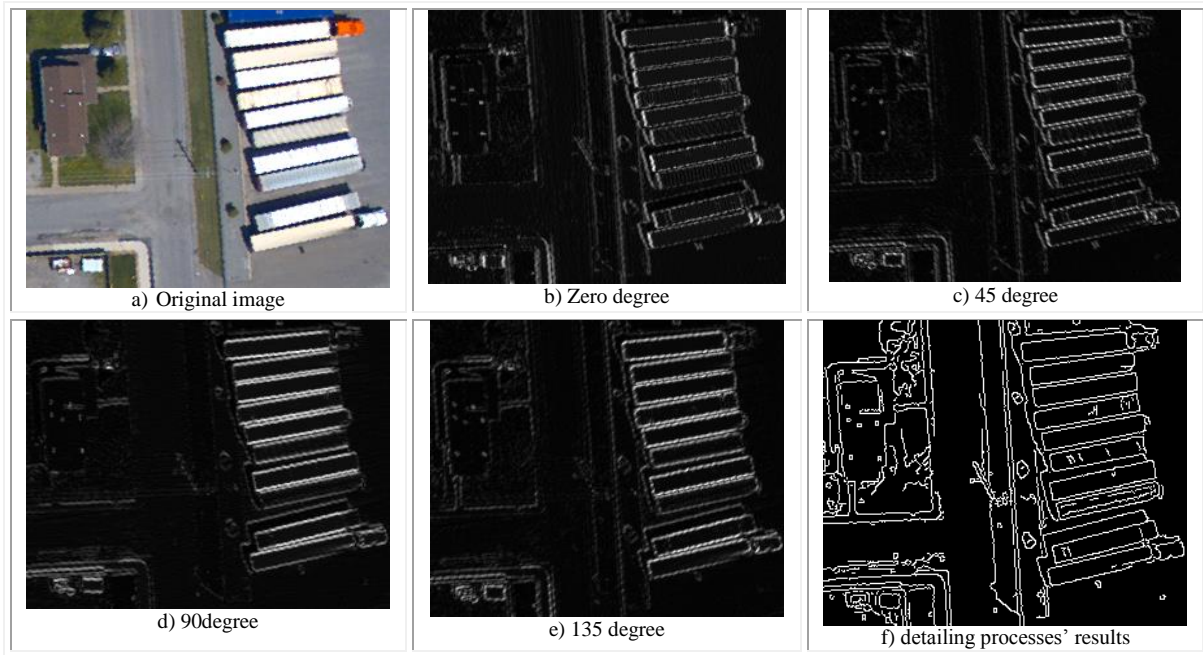


FIGURE 6 2-D Gabor filter used in image edge detecting

4.2 ANALYSIS OF ROC CURVE

ROC curve (receive operating characteristic curve) can be well applied to evaluate different edges' detection operator and detection accuracy.

TABLE 2 Four results of logogram and meaning of edge detecting

logogram	meaning
EE	Edge points correctly detected as edge point
ENE	edge point but erroneously detected as non-edge point
NEE	non-edge point but erroneously detected as edge point
NENE	non-edge point correctly detected as non-edge point

For every pixel in the image, there are four possible kinds of detecting results, respectively named in the Table 2 above.

Therefore, ROC curves used to reflect the relationship between positive edge detection operator class (*TP*, true-positive) and negative category (*FP*, false-positive), *TP* and *FP* can be defined as follows:

$$TP = \frac{n_{EE}}{n_{EE} + n_{ENE}}, \quad FP = \frac{n_{NEE}}{n_{NEE} + n_{NENE}}, \quad (7)$$

where the above equation, n_{EE} , n_{ENE} , n_{NEE} , n_{NENE} is the number of the four results.

Figure 7 shows the ROC curve of Canny operator, Sobel operator and the proposed GW algorithm, known as *FP* when taken from 0 to 0.12, *TP* was significantly higher than the value of the proposed algorithm Canny operator, *FP* is taken from 0 to 0.5, two algorithms proposed by this paper are better than Canny operator. When the *FP* is higher than 0.5, the algorithms mentioned by this paper are either better than Canny operator or equal to it.

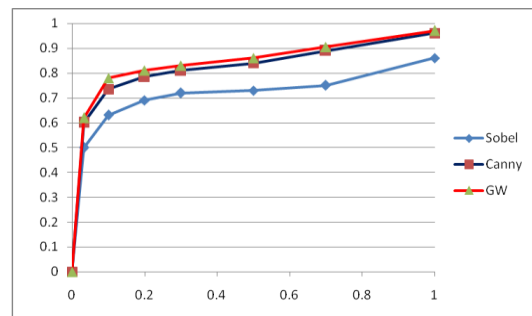


FIGURE 7 GW, Canny and Sobel operators ROC curve

5 Conclusions

With the features of large amount of data and complex landmark, remote sensing images need a higher requirement for edge detection operator. Due to the limitations of grads operator and Canny operator in edge detection, this paper presents an edge detection method based on 2-D Gabor wavelet real part and the experimental analysis shows this method was better on edge detection. However, the method of calculating takes more time to get a result. It will lead to more time-consuming, consequently in further studies, the degree of automation should be enhanced in edge detection.

Acknowledgments

This work was supported by Zhejiang Provincial Natural Science Foundation of China (No.LQ12D01001, No.LQ12F03001), Natural Science Foundation of China (No.61203360), Ningbo City Natural Science Foundation of China (No.2012A610043, No.2012A610009).

References

- [1] Lades M, Vorbruggen J C, Buhmann J, Lange J, von der Malsburg C, Wurtz R P, Konen W 1993 *IEEE Transactions on Computers* **42**(3) 300-11
- [2] Wang X, Chen X, Jin M 2005 Application of line segment extraction to recognize buildings in high-resolution remote sensing images *Journal of Computer Aided Design and Graphics* **17**(5) 928-34
- [3] Lee T S 1996 *IEEE Transactions on Pattern Analysis and Machine Intelligence* **18**(10) 959-71
- [4] Ma W Y, Manjunath B S 1997 Edge flow: a framework of boundary detection and image segmentation *Proceedings of the IEEE Conference on Computer Vision and Pattern Recognition 1997* San Juan Puerto Rico 744-9
- [5] Nevatia R, Lin C, Huertas A 1997 A System for Building Detection from Aerial Images *In Automatic Extraction of Man-Made Objects from Aerial and Space Images*, edited by Gruen A, Kuebler O, Agouris P 1997
- [6] Guan Y P 2008 Automatic Extraction of lips Based on Multi-scale Wavelet Edge Detection *IET Computer Vision* **2**(1) 23-33
- [7] Fu Z, Tong C, Yan H Fan Z 2010 Parallel Gabor Wavelet Transform for Edge detection *International Conference on Internet Technology and Applications* August 2010 Wuhan China 1-3
- [8] Tomasi C, Manduchi R 1998 Bilateral Filtering for Gray and Color Images *Proceedings of the 1998 IEEE International Conference on Computer Vision* Bombay India 839-46
- [9] Yang Q, Li J 1999 Using the Tag Growth Extracting Line Segments from the Edge Image *Journal of Shanghai Jiaotong University* **33**(4) 466-8

Author



Chunya Tong, born in July, 1980, China

University studies: PhD degree in Photogrammetry and Remote Sensing from Wuhan University, Wuhan, China in 2011.

Scientific interest: remote sensing image processing.